JOURNAL OF APPLIED CRYSTALLOGRAPHY
ISSN 1600-5767

Niggli reduction and Bravais lattice determination

Hong-Long Shi[a]* and Zi-An Li[b]

[a]School of Science, Minzu University, 27 Zhang Guancun South Avenue, Haidian District, Beijing, 100081, People's Republic of China, and [b]School of Physical Science and Technology, Guangxi University, No. 100 Daxuedong Road, Xixiangtang District, Nanning, Guangxi, 530004, People's Republic of China. *Correspondence e-mail: honglongshi@outlook.com

Received 14 October 2021
Accepted 13 December 2021

Edited by S. Boutet, SLAC National Accelerator Laboratory, Menlo Park, USA

Keywords: Niggli reduction; reduced cells; symmetry constraints; Bravais lattices; unit cells.

Supporting information: this article has supporting information at journals.iucr.org/j

A new algorithm has been developed and coded in *DigitalMicrograph* (*DM*) to reduce a three-dimensional primitive cell to the Niggli cell and further convert to the Bravais-lattice unit cell. The core of this algorithm is the calculation of the three shortest non-coplanar vectors to compose the reduced cell. The reduced cell is converted into the real-space reduced cell and then to the Bravais-lattice unit cell. The symmetry-constrained unit cell is, in turn, converted back into the real-space reduced cell, the reciprocal reduced cell and the reciprocal primitive cell. The *DM* package demonstrates superior numerical stability and can tolerate large uncertainties in the experimentally measured input primitive cell, making it especially suitable for electron diffraction analysis. Additionally, the *DM* package can be used to calculate various crystallographic parameters including Bravais-lattice plane indices, zone-axis indices, tilt angles and the radius of the high-order Laue zone ring, thus facilitating the correct determination of the Niggli cell and the Bravais lattice.

1. Introduction

The fundamental step for *ab initio* new crystal structure determination (Putz *et al.*, 1999; Le Bail *et al.*, 1988; Young, 1993) is determining the Bravais-type unit-cell parameters of a crystal. The unit cell can be uniquely obtained once the primitive cell that can be constructed from X-ray, neutron or electron diffraction measurements (Pecharsky & Zavalij, 2003; Fultz & Howe, 2013; Williams & Carter, 2009) is reduced to the Niggli cell (Santoro & Mighell, 1970; Gruber, 1973; de Wolff, 2006), because the Niggli cell provides a unique description of a lattice and is defined independently of the lattice symmetry. This is well documented in *International Tables for Crystallography*, Vol. A (de Wolff, 2006).

In 1928, Niggli put forward a set of conditions that produce a unique choice of basis vectors of a lattice. Subsequently, Křivý & Gruber (1976) presented a numerical algorithm for the Niggli reduction, and later the number of iterations of this algorithm was optimized by Zuo *et al.* (1995). Křivý and Gruber use the following notation in the description of the reduction algorithms:

$$\begin{aligned} A &= \mathbf{a}\cdot\mathbf{a} = a^2, \quad B = \mathbf{b}\cdot\mathbf{b} = b^2, \quad C = \mathbf{c}\cdot\mathbf{c} = c^2, \\ D &= 2\mathbf{b}\cdot\mathbf{c} = 2bc\cos\alpha, \quad E = 2\mathbf{a}\cdot\mathbf{c} = 2ac\cos\beta, \\ F &= 2\mathbf{a}\cdot\mathbf{b} = 2ab\cos\gamma, \end{aligned} \tag{1}$$

where **a**, **b** and **c** are the basis vectors of a cell with parameters a, b, c, α, β and γ; the parameters A, B, C, D, E and F represent the Niggli-matrix elements S_{ij}.

In real-world applications, two major problems exist during the reduction procedure. The first problem is the treatment of

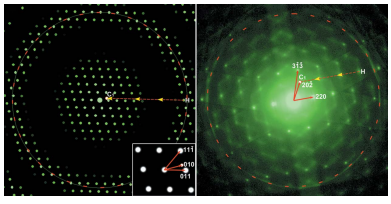

rounding errors, since algorithms implemented using finite-precision floating-point algebra can result in infinite loops when the rounding errors are improperly treated (*e.g.* irrational numbers). This first problem was addressed by Grosse-Kunstleve *et al.* (2004) by introducing a tolerance factor to improve the numerical stability of algorithms. The second problem is the treatment of the measurement errors of the experimentally measured input cell (Yang *et al.*, 2017). These cells with errors generate matrix elements S_{ij} with uncertainties that can be further magnified and propagated to the successive steps of reduction, finally resulting in a reduced cell with a large uncertainty that makes correct determination of the Bravais lattice very difficult.

Electron diffraction is a powerful technique to determine crystal structure at the nanoscale (Zheng *et al.*, 2014; Wen *et al.*, 2018; Sheng *et al.*, 2016), and the 3D reciprocal cell can be determined directly from electron diffraction patterns (Shi & Li, 2021; Jiang *et al.*, 2011; Li, 2019; Zhao *et al.*, 2008; Zou *et al.*, 2004). However, the primitive cell measured from an electron diffraction pattern suffers from a poor measurement precision because the measured d spacings exhibit around 1% error, resulting from the diffraction distortions of the electromagnetic lens and the uncertainty of the camera length of the transmission electron microscope (Mitchell & Van den Berg, 2016; Hou & Li, 2008). Moreover, the measurement error of interzonal angles of a tilt series can be up to a few degrees. Although the relation between the Niggli cell and the Bravais lattice is definitive, errors in the experimentally observed cell will propagate to the Niggli cell, making the conversion of the Niggli cell into the Bravais lattice very difficult.

Here, we present an alternative algorithm and a corresponding *DigitalMicrograph* (*DM*; Gatan, 2019) package, *Niggli Reduction Tools*, to calculate the Niggli cell and convert the Niggli cell into the Bravais lattice. In the new algorithm, parameters $\varepsilon_{1\text{–}3}$ are introduced as tolerance factors for the measurement errors of the basis-vector lengths. Such treatment can tolerate large experimental error and achieve better numerical stability. The parameters $\varepsilon_{\rm d}$ and $\varepsilon_{\rm A}$ define errors on the lengths and angles of the Bravais-lattice unit cell. Additionally, symmetry constraints on the determined Bravais cell are used to evaluate the measurement errors of the observed cell in the electron diffraction pattern. The *DM* package can also be used to calculate the Bravais-lattice plane indices, zone-axis indices and tilt angles, as well as the radius of the high-order Laue zone (HOLZ) ring of the electron diffraction pattern. The robustness of the new algorithm for converting the Niggli cell to the Bravais lattice will be demonstrated and discussed.

2. Algorithms

2.1. Fundamentals of the Niggli reduction and the unit-cell determination

Since a primitive cell has lattice points only at its vertices, all lattice points appear at the vertices of the collection of the identical primitive cells of the lattice. This means that each point of the lattice can be retrieved from any other lattice point by a vector sum of cell edges of a primitive cell.

Let vectors **a**, **b** and **c** be the edges of a primitive cell. The translation vector **t** of the lattice point at (u, v, w) can be described as $\mathbf{t} = u\mathbf{a} + v\mathbf{b} + w\mathbf{c}$. If we start with an arbitrary primitive cell with edges **a**, **b** and **c**, and wish to obtain a Niggli reduced cell with edges $\mathbf{t}_1$, $\mathbf{t}_2$ and $\mathbf{t}_3$, the three edges of the new cell can be expressed in terms of the old ones as $\mathbf{t}_i = u_i\mathbf{a} + v_i\mathbf{b} + w_i\mathbf{c}$, where the subscript $i = 1, 2, 3$. The indices (u_i, v_i, w_i) are small integers. The edge length of the new cell can be determined by the scalar product with itself, $t_i^2 = \mathbf{t}_i \cdot \mathbf{t}_i$; and the angles between two edges of the new cell can be calculated by using the relation $\cos(\mathbf{t}_i, \mathbf{t}_j) = \mathbf{t}_i \cdot \mathbf{t}_j/(|\mathbf{t}_i||\mathbf{t}_j|)$. In this way, the three shortest non-planar vectors compose the Niggli reduced cell with parameters a_0^*, b_0^*, c_0^*, α_0^*, β_0^* and γ_0^*.

The obtained Niggli reduced cell described in the reciprocal space can be transformed into a real-space reduced cell (a_0, b_0, c_0, α_0, β_0 and γ_0) through the relationship between the real and reciprocal lattice. The real-space reduced cell can then be transformed into the Bravais-lattice unit cell (unit cell; a, b, c, α, β and γ) based on the conditions of the Niggli matrix elements S_{ij} as reported in *International Tables for Crystallography*, Vol. A.

Errors of the Niggli reduced cell propagated from the reciprocal primitive cell (or the input cell) can propagate to the Bravais-lattice unit cell. These errors can be evaluated and corrected by applying symmetry constraints on the standard Bravais lattice: (1) Edges and angles of the obtained unit cell can be constrained as the symmetry-constrained unit cell (abbreviated as the sym. unit cell) to satisfy the symmetry of the Bravais lattice. (2) In turn, the symmetry-constrained unit cell is inversely transformed into the real-space reduced cell, the reciprocal reduced cell and the reciprocal primitive cell. The obtained primitive cell is a symmetry-constrained cell that can be used to evaluate and correct the errors of the input cell, or even to perform refinement of the lattice parameters from experimental electron diffraction data.

2.2. Description of the program

The package *Niggli Reduction Tools* is based on the *DigitalMicrograph* software, whose language is similar to C or C++. The package grants permission to copy, use or modify the code for any purpose under a license.

2.2.1. Distribution and installation. The package is freely available by email (honglongshi@outlook.com) and as supporting information to this article, and the *DigitalMicrograph* software is available at https://www.gatan.com/products/tem-analysis/gatan-microscopy-suite-software.

There are two files in this package:

(i) `NiggliReduction.gtk`: a compiled package of *Niggli Reduction Tools*.

(ii) `Tutorial.pdf`: a concise help file.

To install the package, the file `NiggliReduction.gtk` should be copied to `...\Gatan\DigitalMicrograph\PlugIns`. A new menu 'ED Tools / Niggli Reduction Tools' will be built on the menu bar of *DigitalMicrograph*. Clicking

the menu 'ED Tools / Niggli Reduction Tools' will launch the graphical user interface (GUI) [Fig. 1(*b*)].

2.2.2. Software overview. *Niggli Reduction Tools* can reduce any 3D reciprocal primitive cell to the Niggli cell and determine the Bravais-lattice unit cell, as shown in Fig. 1(*b*). The GUI has four sections: (1) the 'Parameters' box defines the input cell, the index range 'N', and the tolerance factors 'eps 1~3' and 'eps d/A'; (2) the 'Reduced Cell List' box lists the three shortest non-planar vectors within the tolerance factors eps 1~3; (3) the 'Unit Cell List' box lists the possible Bravais lattices within the tolerance of eps d/A; and (4) the 'Results' box outputs a concise list of derived cells and other useful parameters.

The parameters of the package are defined as follows:

Input cell: defines the measured reciprocal primitive cell. The unit of the input cell can be Å^{-1} or nm^{-1}. If a real-space cell is input, it can be converted into a reciprocal cell by simultaneously clicking the 'Alt' key and the 'Calc.' button.

eps 1~3: defines the factors ε_{1-3} to give the tolerance lengths of the shortest vectors $\mathbf{t}_1$, $\mathbf{t}_2$ and $\mathbf{t}_3$. This mainly depends on the measurement error Δp (typically, 1–5 pixels) and the resolution r of the examined electron diffraction pattern (or the image scale, *e.g.* nm^{-1} per pixel), and $\varepsilon_{1-3} = \Delta p\, r$.

eps d/A: defines the tolerance factors ε_d (the unit is ångström) and ε_A (the unit is degree) of the unit cell in matching the Bravais lattice.

N: defines the range of indices (u, v, w) used in searching for the shortest vectors.

The algorithm of *Niggli Reduction Tools* is as follows:

S1. Input a reciprocal primitive cell: a^*, b^*, c^*, α^*, β^*, γ^*.

S2. For $-N \le (u, v, w) \le N$, calculate the length of the vector $\mathbf{t}_{u,v,w}$.

S3. Find the first three minima t_{10}, t_{20} t_{30}.

S4. If $t_{10} < t_i < t_{10} + \varepsilon_1$, find the collection of the first minima and create the vector $\mathbf{t}_1$.

S5. If $t_{20} < t_i < t_{20} + \varepsilon_2$, find the collection of the second minima (non-collinear with $\mathbf{t}_1$) and create the vector $\mathbf{t}_2$.

S6. If $t_{30} < t_i < t_{30} + \varepsilon_3$, find the collection of the third minima (non-coplanar with $\mathbf{t}_1$ and $\mathbf{t}_2$) and create the vector $\mathbf{t}_3$. The three vectors $\mathbf{t}_1$, $\mathbf{t}_2$ and $\mathbf{t}_3$ compose the reciprocal reduced cell.

S7. Convert the reciprocal reduced cell to the real reduced cell.

S8. Convert the real reduced cell into the Bravais-lattice unit cell within the tolerance of ε_d and ε_A and determine the symmetry-constrained unit cell.

S9. Convert the constrained unit cell to the real reduced cell.

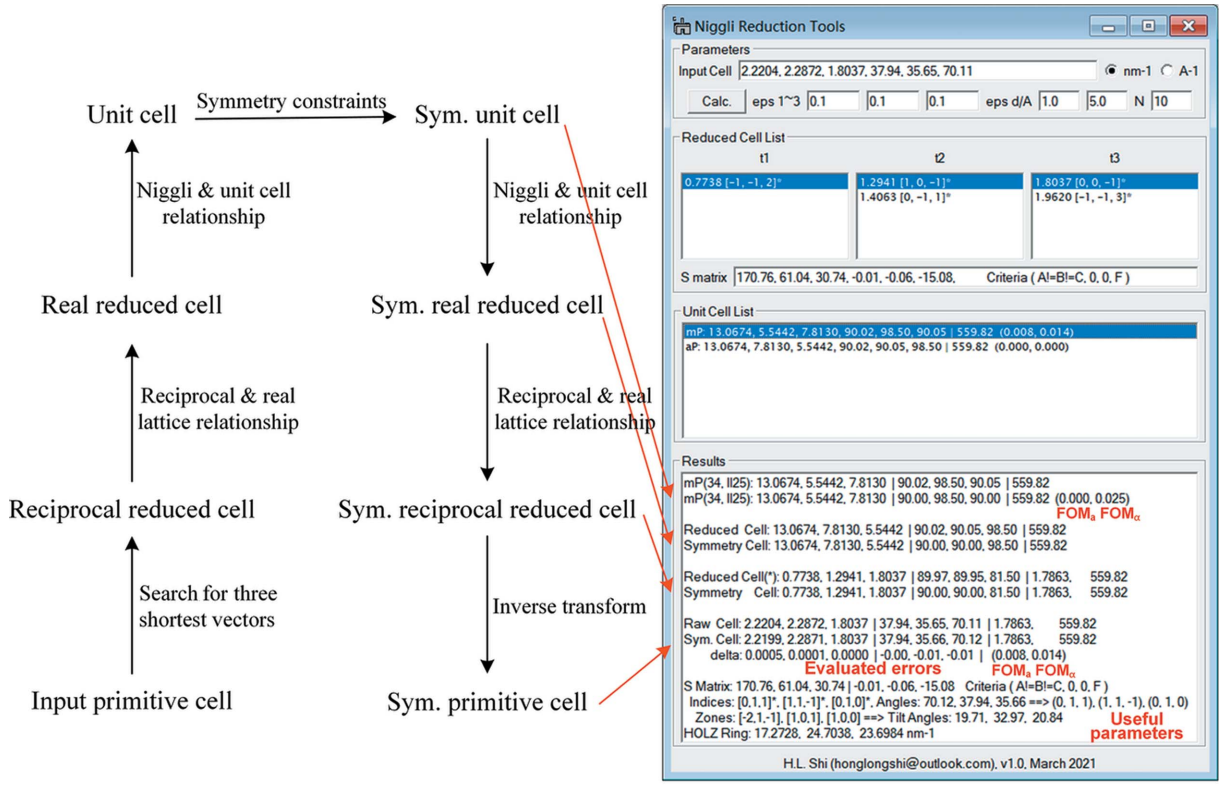

(*a*) (*b*)

Figure 1
(*a*) A flow chart of *Niggli Reduction Tools*, and (*b*) a screen capture of the graphical user interface of the package. The parameters 'eps 1~3' define the tolerance of the edges of the input cell; 'eps d/A' are the errors of the edges and angles of the Bravais lattice; and 'N' is the range of indices. From top to bottom in the 'Results' box are pairs of the unit cell, the real reduced cell, the reciprocal reduced cell and the reciprocal primitive cell (raw cell), as well as figures of merit FOM_a and FOM_α of the unit cell and the raw cell, the evaluated errors of the raw cell 'delta', the *S* matrix and the Bravais criteria, the Bravais-lattice-plane indices, the zone-axis indices, the tilt angles, and the radius of the HOLZ ring.

S10. Convert the real reduced cell to the reciprocal reduced cell.

S11. Convert the reciprocal reduced cell to the reciprocal primitive cell and calculate other parameters.

Fig. 1(*a*) shows the workflow of the package *Niggli Reduction Tools*. After the parameters of the reciprocal cell (a^*, b^*, c^*, α^*, β^*, γ^*) have been input, the three basis vectors ($\mathbf{a}^*$, $\mathbf{b}^*$, $\mathbf{c}^*$) of the input cell are created in the orthogonal coordinate system as follows (note: if the input cell is a real-space cell, press the 'Alt' key and click the 'Calc.' button to convert it to the reciprocal cell):

$$\begin{aligned}\mathbf{a}^* &= (a^*,\ 0,\ 0),\\ \mathbf{b}^* &= (b^*\cos\gamma^*,\ b^*\sin\gamma^*,\ 0),\\ \mathbf{c}^* &= \left(c^*\cos\beta^*,\ -c^*\sin\beta^*\frac{\cos\beta^*\cos\gamma^*-\cos\alpha^*}{\sin\beta^*\sin\gamma^*},\right.\\ &\qquad \left.\frac{V^*}{a^*b^*\sin\gamma^*}\right),\end{aligned} \tag{2}$$

where V^* is the volume of the input cell. The vector length t of each index (u, v, w) within the index range of $\pm N$ is then calculated; and the three minima (t_{10}, t_{20}, t_{30}) of the t_i list can be determined.

Next, the first minimum t_1 within the range $t_{10} \le t_i \le t_{10} + \varepsilon_1$ is found and the vector t_1 is created; the second minimum t_2 (nonlinear with the vector $\mathbf{t}_1$) within the range $t_{20} \le t_i \le t_{20} + \varepsilon_2$ is found and the vector $\mathbf{t}_2$ created; and the third minimum t_3 (non-coplanar with vectors $\mathbf{t}_1$ and $\mathbf{t}_2$) within the range $t_{30} \le t_i \le t_{30} + \varepsilon_3$ is found and the vector $\mathbf{t}_3$ created. Three lists of t_1, t_2 and t_3 that compose the reduced cell are found in this way and displayed in the 'Reduced Cell List' box [Fig. 1(*b*)].

After the reduced cell has been chosen by successively clicking the list t_1, t_2 and t_3, it will be converted into the real reduced cell (a_0, b_0, c_0, α_0, β_0 and γ_0). The basis vectors ($\mathbf{a}_0$, $\mathbf{b}_0$, $\mathbf{c}_0$) of the reduced cell are created in the orthogonal coordinate system, written as the matrix A in equation (3); and the transformation matrix M can be found in *International Tables for Crystallography*, Vol. A (de Wolff, 2006). In this way, the real reduced cell is transformed into 44 Bravais-lattice unit cells U by matrix multiplication of the matrices M and A:

$$U = MA, \quad M = \begin{bmatrix} m_{11} & m_{12} & m_{13}\\ m_{21} & m_{22} & m_{23}\\ m_{31} & m_{32} & m_{33}\end{bmatrix},$$

$$A = \begin{bmatrix} a_0 & 0 & 0\\ b_0\cos\gamma_0 & b_0\sin\gamma_0 & 0\\ c_0\cos\beta_0 & -c_0\sin\beta_0\dfrac{\cos\beta_0\cos\gamma_0-\cos\alpha_0}{\sin\beta_0\sin\gamma_0} & \dfrac{V_0}{a_0b_0\sin\gamma_0}\end{bmatrix}. \tag{3}$$

The lattice parameters are determined from the elements of the matrix U as follows:

$$\begin{aligned} a &= \left(u_{11}^2+u_{12}^2+u_{13}^2\right)^{1/2},\\ b &= \left(u_{21}^2+u_{22}^2+u_{23}^2\right)^{1/2},\\ c &= \left(u_{31}^2+u_{32}^2+u_{33}^2\right)^{1/2},\\ \alpha &= \cos^{-1}\left(\frac{u_{31}u_{21}+u_{32}u_{22}+u_{33}u_{23}}{bc}\right),\\ \beta &= \cos^{-1}\left(\frac{u_{11}u_{31}+u_{12}u_{32}+u_{13}u_{33}}{ac}\right),\\ \gamma &= \cos^{-1}\left(\frac{u_{11}u_{21}+u_{12}u_{22}+u_{13}u_{23}}{ab}\right).\end{aligned} \tag{4}$$

Only those cells whose edge and angle errors fall in the range of ε_d and ε_A are listed in the 'Unit Cell List' box [Fig. 1(*b*)]. When one cell is chosen from the 'Unit Cell List' box, the selected unit cell will be constrained according to the symmetry of the Bravais lattice. The symmetry-constrained unit cell is further inversely converted into the real reduced cell, the reciprocal reduced cell and the reciprocal primitive cell. A concise result list of cells is displayed in the 'Results' box; more details of the results are output in the 'Results' window of the *Digital Micrograph* software.

Some additional useful parameters are calculated to help choose the correct Niggli cell and Bravais lattice: (1) errors between the observed cell and the symmetry-constrained cell are evaluated; (2) the S matrix and the Bravais-lattice criteria are live displayed when choosing one cell in the 'Unit Cell List' box; (3) the Bravais-lattice plane indices, the zone-axis indices and tilt angles are calculated; and (4) the radius of the HOLZ ring is derived.

3. Illustrative examples

To demonstrate the use of the *Niggli Reduction Tools* package, two examples are given here. The first is to reduce a cell with small errors constructed from a simulated electron diffraction pattern of an $La_2(Ti_2O_7)$ crystal oriented at $[\bar{2}1\bar{1}]$. The second is to reduce a cell with large uncertainties determined from the experimental electron diffraction pattern of a silicon crystal.

3.1. Determination of the reduced cell and unit cell of a low-symmetry lattice (small errors)

The input cell for the Niggli reduction is obtained by reconstructing the 3D reciprocal cell from a simulated electron diffraction pattern of the monoclinic structure $La_2(Ti_2O_7)$ with sub-pixel measurement error (scale = 0.019424 nm^{-1} per pixel). The cell parameters described in the reciprocal space are a^* = 2.2204, b^* = 2.2872, c^* = 1.8037 nm^{-1}, α^* = 37.94, β^* = 35.65, γ^* = 70.11°, as shown in Fig. 2(*a*). After inputting the cell parameters and clicking the 'Calc.' button, we obtain the lists of t_1, t_2 and t_3 in the 'Reduced Cell List' box (ε_{1-3} = 0.1 nm^{-1} and N = 10), as shown in Fig. 1(*b*). Here, we select the reduced cell with the shortest edges (the topmost one, a_0^* = 0.7738, b_0^* = 1.2941, c_0^* = 1.8037 nm^{-1}, α_0^* = 89.97, β_0^* = 89.95, γ_0^* = 81.50°); according to the real–reciprocal relationship of the lattice, the real reduced cell is calculated to be a_0 = 13.0674, b_0 = 7.8130, c_0 = 5.5442 Å, α_0 = 90.02, β_0 = 90.05, γ_0 = 98.50° with the Niggli-matrix elements of A = 170.76, B = 61.04, C = 30.74,

Table 1
List of the determined cells and the symmetry-constrained cells of two examples: (1) the input cell with small errors created from a low-symmetry lattice of $La_2(Ti_2O_7)$, and (2) the input cell with large errors reconstructed from a high-symmetry lattice of single-crystal silicon.

The units are nm^{-1} and Å for edges of the reciprocal-space cells and real-space cells, respectively.

(1) $La_2(Ti_2O_7)$ oriented at $[\bar{2}1\bar{1}]$ (PDF No. 81-1066, $P2_1$, $a = 7.812$, $b = 5.544$, $c = 13.010$ Å, $\alpha = 90.00$, $\beta = 98.66$, $\gamma = 90.00°$).

	Determined cell	Symmetry constrained cell
Input cell	2.2204, 2.2872, 1.8037, 37.94, 35.65, 70.11	2.2199, 2.2871, 1.8037, 37.94, 35.66, 70.12
Reduced cell*	0.7738, 1.2941, 1.8037, 89.97, 89.95, 81.50	0.7738, 1.2941, 1.8037, 90.00, 90.00, 81.50
Reduced cell	13.0674, 7.8130, 5.5442, 90.02, 90.05, 98.50	13.0674, 7.8130, 5.5442, 90.00, 90.00, 98.50
Unit cell	13.0674, 5.5442, 7.8130, 90.02, 98.50, 90.05	13.0674, 5.5442, 7.8130, 90.00, 98.50, 90.00

(2) Single-crystal silicon oriented at $[\bar{3}3\bar{4}]$ (PDF No. 77-2108, $Fd\bar{3}m$, $a = b = c = 5.42$ Å, $\alpha = \beta = \gamma = 90.00°$).

	Determined cell	Symmetry constrained cell
Input cell	5.2083, 7.9618, 5.1259, 13.30, 60.94, 71.93	5.2186, 8.0424, 5.2186, 13.26, 60.00, 71.07
Reduced cell*	3.1020, 3.1987, 3.2412, 110.94, 107.13, 108.88	3.1957, 3.1957, 3.1957, 109.47, 109.47, 109.47
Reduced cell	3.8466, 3.8169, 3.7298, 59.95, 62.34, 61.28	3.8324, 3.8324, 3.8324, 60.00, 60.00, 60.00
Unit cell	5.3133, 5.4598, 5.4866, 91.56, 92.64, 88.87	5.4199, 5.4199, 5.4199, 90.00, 90.00, 90.00

$D = -0.01$, $E = -0.06$ and $F = -15.09$. Subsequently, the real reduced cell is converted into the Bravais lattices that are listed in the 'Unit Cell List' box only when the differences of lengths and angles of the cell fall in the range of ε_d and ε_A. In this example, two Bravais lattices, mP and aP, are listed. Requiring that the matrix elements of the reduced cell meet the conditions $A \neq B \neq C$, $D = E = 0$ and $F \neq 0$ (No. 34, II25), the monoclinic structure mP is selected. The obtained Bravais lattice is mP, *i.e.* it must satisfy the symmetry of the monoclinic crystal system ($a \neq b \neq c$, $\alpha = \gamma = 90°$). After applying the symmetry constraints to the selected unit cell, the parameters of the cell become $a = 13.0674$, $b = 5.5442$, $c = 7.8130$ Å, $\alpha = 90.00$, $\beta = 98.50$, $\gamma = 90.00°$. In turn, the symmetry-constrained unit cell is inversely converted into the real reduced cell, the reciprocal reduced cell and the reciprocal primitive cell (detailed parameters are listed in Table 1). The symmetry-constrained reciprocal primitive cell is $a^* = 2.2199$, $b^* = 2.2871$, $c^* = 1.8037$ nm^{-1}, $\alpha^* = 37.94$, $\beta^* = 35.66$, $\gamma^* = 70.12°$. The errors between the input cell and the symmetry-constrained cell are evaluated to be $\Delta a^* = 0.0005$, $\Delta b^* = 0.0001$, $\Delta c^* = 0.0000$ nm^{-1}, $\Delta\alpha^* = 0.00$, $\Delta\beta^* = -0.01$, $\Delta\gamma^* = -0.01°$, respectively.

For convenience to evaluate the candidate Niggli cell and the unit cell, *Niggli Reduction Tools* provides additional useful parameters:

(1) 'S matrix' and 'Criteria': the S matrix of the reduced cell and the Bravais criteria for transforming the reduced cell to the unit cell.

(2) 'Indices' and 'Angles': the lattice-plane indices of the diffraction spots indicated by the three basis vectors of the input cell, and the angles between the vectors. The lattice-plane indices inherit the symmetry of the unit cell and hence can be used to select the reduced cell and the unit cell in the 'Reduced Cell List' and the 'Unit Cell List'; the derived angles between the vectors can be compared with the measured values in the tilt series experiment.

(3) 'Zones' and 'Tilt Angles': the zone-axis indices of the diffraction patterns for constructing the three-dimensional reciprocal primitive cell, and the tilt angles between zone axes. The tilt angles can be directly compared with the angles calculated from 'Tilt X' and 'Tilt Y' of the transmission electron microscope.

(4) 'HOLZ Ring': the radii of the HOLZ rings of three zone-axis patterns which can be compared with the measured ones.

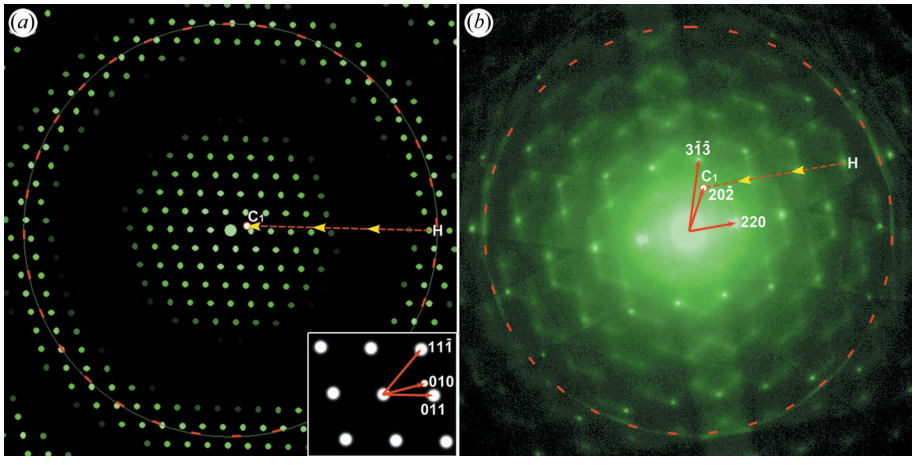

Figure 2
(*a*) The simulated electron diffraction pattern of $La_2(Ti_2O_7)$ oriented at $[\bar{2}1\bar{1}]$. The inset is the enlarged zero-order Laue pattern. (*b*) The experimental electron diffraction pattern of single-crystal silicon oriented at $[\bar{3}3\bar{4}]$. The high-order Laue ring is marked as a dashed ring, and the high-order Laue diffraction spot for reconstructing the reciprocal lattice is marked H, which is vector-shifted to C_1 in the zero-order Laue pattern.

In this illustration, the S matrix of the reduced cell, (170.76, 61.04, 30.74, −0.01, −0.06, −15.08), fully satisfies the criteria ($A \neq B \neq C$, $D = E = 0$, $F \neq 0$). The lattice-plane indices of the three diffraction spots indicated by the basis vectors are $(011)_{a^*}$, $(11\bar{1})_{b^*}$ and $(010)_{c^*}$, respectively. Therefore, the interplanar angles are 70.12, 37.94 and 35.66° between the vectors $\mathbf{a}^*$ and $\mathbf{b}^*$, $\mathbf{b}^*$ and $\mathbf{c}^*$, and $\mathbf{c}^*$ and $\mathbf{a}^*$, respectively (versus 70.11°, the measured angle based on the one-pattern method). The zone axis of the examined pattern is $[\bar{2}1\bar{1}]$, and the radius of the HOLZ ring is calculated to be 17.2712 nm^{-1} versus 17.2728 nm^{-1} for the measured one. The small differences between the observed

Table 2
Four equivalent reduced cells in the case of the silicon single crystal.

The units are nm^{-1} and Å for edges of the reciprocal-space cells and real-space cells, respectively.

Reciprocal vectors	Bravais-lattice planes	Reduced cell	Unit cell
$[0\bar{1}2]^*$, $[0\bar{1}1]^*$, $[13\bar{5}]^*$	(220), (3$\bar{1}\bar{3}$), (20$\bar{2}$)	3.1020, 3.1987, 3.2412, 110.94, 107.13, 108.88	5.3133, 5.4598, 5.4866, 91.56, 92.64, 88.87
$[0\bar{1}2]^*$, $[0\bar{1}1]^*$, $[\bar{1}\bar{1}2]^*$	(02$\bar{2}$), (3$\bar{1}\bar{3}$), (20$\bar{2}$)	3.1020, 3.1987, 3.2563, 108.56, 109.97, 108.88	5.4866, 5.4598, 5.3133, 91.13, 92.64, 88.44
$[0\bar{1}2]^*$, $[13\bar{5}]^*$, $[\bar{1}\bar{1}2]^*$	(02$\bar{2}$), (33$\bar{1}$), (220)	3.1020, 3.2412, 3.2563, 111.32, 109.97, 107.13	5.4866, 5.3133, 5.4598, 91.13, 91.56, 87.36
$[0\bar{1}1]^*$, $[13\bar{5}]^*$, $[\bar{1}\bar{1}2]^*$	($\bar{2}$02), ($\bar{3}$3$\bar{1}$), ($\bar{2}\bar{2}$0)	3.1987, 3.2412, 3.2563, 111.32, 108.56, 110.94	5.3133, 5.4866, 5.4598, 88.44, 88.87, 87.36

cell and the determined cell, as well as the comparison between the measured values and calculated ones based on the symmetry-constrained unit cell, suggest that the determined Niggli cell and the Bravais-lattice unit cell are valid.

In this example, a low-symmetry anisotropic crystal $La_2(Ti_2O_7)$ is examined, and the top three shortest vectors in the list of t_1, t_2, and t_3 always compose the Niggli reduced cell. However, a high-symmetry crystal often generates multiple equivalent vectors; and the errors of the input cell make these equivalent vectors different, which complicates the procedure of choosing the reduced cell.

3.2. Determination of the reduced cell and the unit cell of a high-symmetry lattice (large errors)

Here, we will discuss a high-symmetry case and an input cell with large uncertainties (*e.g.* 1–2 pixels, 0.057783 nm^{-1} per pixel). The primitive cell was extracted from the experimental electron diffraction pattern of a silicon single crystal [Fig. 2(*b*)]. The parameters of the input cell are $a^* = 5.2083$, $b^* = 7.9618$, $c^* = 5.1259$ nm^{-1}, $\alpha^* = 13.30$, $\beta^* = 60.94$, $\gamma^* = 71.93°$. After the Niggli reduction, the three non-planar shortest vectors $[0\bar{1}2]^*$, $[0\bar{1}1]^*$ and $[13\bar{5}]^*$ produce the candidate reduced cell with parameters $a_0^* = 3.1020$, $b_0^* = 3.1987$, $c_0^* = 3.2412$ nm^{-1}, $\alpha_0^* = 110.94$, $\beta_0^* = 107.13$, $\gamma_0^* = 108.88°$. Subsequently, the reduced cell is converted into the real reduced cell. The *S*-matrix elements of the reduced cell ($A = 14.7961$, $B = 14.5689$, $C = 13.9112$, $D = 7.1280$, $E = 6.6602$, $F = 7.0548$) approximately meet the conditions $A = B = C$ and $D = E = F = A/2$ (cF, 1, I1); thus, the Bravais-lattice unit cell is converted to $a = 5.3133$, $b = 5.4598$, $c = 5.4866$ Å, $\alpha = 91.56$, $\beta = 92.64$, $\gamma = 88.87°$. After applying the symmetry constraints of the cubic crystal system, the symmetry-constrained cell is $a = b = c = 5.4199$ Å, $\alpha = \beta = \gamma = 90.00°$, which in turn is inversely converted to the symmetry-constrained real direct cell, the reciprocal reduced cell and the reciprocal primitive cell (see detailed parameters in Table 1). The symmetry-constrained primitive cell is $a^* = 5.2186$, $b^* = 8.0424$, $c^* = 5.2186$ $Å^{-1}$, $\alpha^* = 13.26$, $\beta^* = 60.00$, $\gamma^* = 71.07°$. The errors between the symmetry-constrained cell and the input cell are evaluated to be $\Delta a^* = -0.0103$, $\Delta b^* = -0.0806$, $\Delta c^* = -0.0927$ nm^{-1}, $\Delta\alpha^* = 0.04$, $\Delta b^* = 0.94$, $\Delta c^* = 0.86°$, respectively. These evaluated errors are entirely consistent with the measurement errors (0.05–0.1 nm^{-1} in length and 1° in angle of the input cell).

Strictly speaking, the determined unit cell in this example is not a cubic phase but a triclinic structure. A similar case is often encountered during electron diffraction analysis because of the large measurement uncertainties of the pattern, which often suffers from image distortions and the unreliable camera length (Mugnaioli *et al.*, 2009; Hou & Li, 2008). Hence, in this work the user-defined parameters ε_{1-3} are introduced to accommodate the measurement uncertainties of the observed cell (or the input cell). Meanwhile, the parameters ε_{1-3} will also result in diverse choices for the Niggli cell. For a high-symmetry lattice and an input cell with large uncertainties, this problem will become more severe. For instance, the measurement errors of the input cell in this example can produce four approximately equivalent reduced cells within the tolerance range of $\varepsilon_{1-3} = 0.1$ nm^{-1} (details are listed in Table 2). Although the listed reduced cells exhibit slight differences and so are converted into different Bravais lattices, these Bravais lattices possess the same symmetry-constrained unit cell with parameters $a = b = c = 5.4199$ Å, $\alpha = \beta = \gamma = 90.00°$. Moreover, the lattice-plane indices corresponding to the reciprocal vectors (listed in Table 2), {220}, {313} and {202}, indicate that these four Niggli cells are indeed equivalent cells. Therefore, to eliminate the ambiguity of choosing the reduced cell for the high-symmetry lattice, we choose each of these approximately equivalent cells in the 'Reduced Cell List' box and check the lattice-plane indices and the symmetry-constrained unit cell, as well as other derived parameters in the 'Results' box.

The other problem in practice is how to choose the correct unit cell from the 'Unit Cell List' box. After a reduced cell has been chosen, it will be converted into 44 Bravais-lattice unit cells based on the relationship between the reduced cell and the unit cell; and only those that match the symmetry of Bravais lattice within the tolerance of ε_d and ε_A will be displayed in the 'Unit Cell List'. Large values of ε_d and ε_A may cause the symmetry of the crystals to be overestimated. Generally, for the electron diffraction technique, the experimental error of the observed cell is larger than that determined in the X-ray or neutron diffraction case; and the deviations of the edges and angles (ε_d and ε_A) of the determined unit cell from the standard cell will be up to 1–2 Å and 5–15°, respectively. To ensure that the correct Bravais lattice is selected in the 'Unit Cell List' box, we suggest choosing the cell with the highest possible symmetry and reasonable evaluated errors, while also checking the Bravais criteria, plane indices, zone-axis indices, tilt angles and HOLZ ring (or symmetry in the HOLZ pattern). In this example, the 'cF' cell with the highest symmetry and reasonable evaluated errors ($\Delta a^* = -0.01$, $\Delta b^* = -0.08$, $\Delta c^* = -0.09$ nm^{-1}, $\Delta\alpha^* = 0.04$, $\Delta\beta^* = 0.94$, $\Delta\gamma^* = 0.86°$ in Table S2 versus the measurement

error of 0.05–0.1 nm^{-1} in length and 1° in angle of the input cell) is the best choice because the other cells, *e.g.* 'hR', 'oI' and 'mC', belong to a sub-cell of 'cF', although it possesses smaller figures of merit (FOM_a = 0.407 and FOM_α = 0.531 in 'mC') than those (FOM_a = 0.992 and FOM_α = 1.020) of the cubic structure.

4. Conclusions

We present a new *DigitalMicrograph* package to calculate the Niggli reduced cell and to determine the Bravais-lattice unit cell. The package can tolerate large uncertainties of the observed cell while obtaining better numerical stability by introducing the factors ε_{1-3}. Some derived characteristic parameters including Bravais-lattice-plane indices, zone-axis indices, tilt angles, the radius of the HOLZ ring and the evaluated errors can be used to facilitate selection of the correct Niggli reduced cell and determine the Bravais lattice. In order to make full use of these parameters to check or verify the determined cell, we suggest to record a high-order Laue pattern [simply focus the electron beam on the specimen and then record the pattern with a short camera length in the parallel-beam mode, or in the convergent beam electron diffraction (CBED) or nanobeam diffraction mode] when you record the electron diffraction pattern for reconstructing the reciprocal cell.

For convenience when choosing the correct Bravais lattice, we summarize three typical cases of reciprocal-cell reconstruction in electron diffraction analysis:

(1) Single-pattern method. The measured parameters in the method are a 2D cell (a^*, b^*, γ^*) and the radius of the HOLZ ring, which can be compared with the derived value R_1 in 'HOLZ Ring'.

(2) Two-pattern method. The measured parameters of the method are two 2D cells (a^*, b^*, c^*, β^*, γ^*) and the tilt angle, which can be compared with the derived value θ_{12} in 'Tilt Angles'. If the HOLZ rings of patterns are measured, they can be compared with the calculated parameters R_1 and R_2 in 'HOLZ Ring'.

(3) Three-pattern method. The measured parameters of the method are three 2D cells (a^*, b^*, c^*, α^*, β^*, γ^*). If the tilt angles are available, the derived values (θ_{12}, θ_{23} and θ_{31} in 'Tilt Angles') can be compared with the measured ones; if the HOLZ rings of the patterns are measured, the calculated parameters (R_1, R_2 and R_3 in 'HOLZ Ring') can assist in choosing the Bravais cell. Moreover, the symmetry of the CBED pattern or the HOLZ pattern can be used to check the determined cell.

Note that the input cell constructed from electron diffraction patterns carries large uncertainties, and the determined reduced cell and the unit cell must be checked by other techniques, *e.g.* the high-order Laue pattern and/or CBED. We suggest to improve the accuracy of the input cell, for example, by strictly calibrating the camera length of the transmission electron microscope and improving the accuracy of the diffraction spot measurement and the reciprocal cell reconstruction.

Acknowledgements

We thank Minting Luo of the Institute of Process Engineering, Chinese Academy of Sciences, for useful discussions.

Funding information

This work was supported by the Fundamental Research Funds for the Central Universities (No. 2020QNPY101) and the Natural Science Foundation of China (grant No. 11974019; grant. No. 11774403).

References

Fultz, B. & Howe, J. M. (2013). *Transmission Electron Microscopy and Diffractometry of Materials.* Berlin, Heidelberg: Springer-Verlag.
Gatan (2019). *DigitalMicrograph Software*, http://www.gatan.com/products/tem-analysis/gatan-microscopy-suite-software.
Grosse-Kunstleve, R. W., Sauter, N. K. & Adams, P. D. (2004). *Acta Cryst.* A**60**, 1–6.
Gruber, B. (1973). *Acta Cryst.* A**29**, 433–440.
Hou, V. D. H. & Li, D. (2008). *Microscopy Today* **16**(3), 36–41.
Jiang, L., Georgieva, D. & Abrahams, J. P. (2011). *J. Appl. Cryst.* **44**, 1132–1136.
Křivý, I. & Gruber, B. (1976). *Acta Cryst.* A**32**, 297–298.
Le Bail, A., Duroy, H. & Fourquet, J. L. (1988). *Mater. Res. Bull.* **23**, 447–452.
Li, X. Z. (2019). *Micron*, **117**, 1–7.
Mitchell, D. R. G. & Van den Berg, J. A. (2016). *Ultramicroscopy*, **160**, 140–145.
Mugnaioli, E., Capitani, G., Nieto, F. & Mellini, M. (2009). *Am. Mineral.* **94**, 793–800.
Pecharsky, V. K. & Zavalij, P. Y. (2003). *Fundamentals of Powder Diffraction and Structural Characterization of Materials.* Boston: Springer US.
Putz, H., Schön, J. C. & Jansen, M. (1999). *J. Appl. Cryst.* **32**, 864–870.
Santoro, A. & Mighell, A. D. (1970). *Acta Cryst.* A**26**, 124–127.
Sheng, H., Zheng, H., Jia, S., Li, L., Cao, F., Wu, S., Han, W., Liu, H., Zhao, D. & Wang, J. (2016). *J. Appl. Cryst.* **49**, 462–467.
Shi, H. L. & Li, Z. A. (2021). *IUCrJ*, **8**, 805–813.
Wen, G., Zheng, H., Wang, K., Cao, F., Zhao, L., Li, L., Wang, J. & Jia, S. (2018). *J. Appl. Cryst.* **51**, 802–808.
Williams, D. B. & Carter, C. B. (2009). *Transmission Electron Microscopy: a Textbook for Materials Science.* New York: Springer US.
Wolff, P. M. de (2006). *International Tables for Crystallography.* Vol. A, *Space Group Symmetry*, edited by Th. Hahn, 1st online ed., ch. 9.2. Chester: International Union of Crystallography.
Yang, Y., Cai, C., Lin, J., Gong, L. & Yang, Q. (2017). *Micron*, **96**, 9–15.
Young, R. A. (1993). *The Rietveld Method.* Oxford University Press.
Zhao, H. S., Wu, D. Q., Yao, J. C. & Chang, A. M. (2008). *Ultramicroscopy*, **108**, 1540–1545.
Zheng, H., Wang, J., Xu, Z. & Gui, J. (2014). *J. Appl. Cryst.* **47**, 879–886.
Zou, X. D., Hovmöller, A. & Hovmöller, S. (2004). *Ultramicroscopy*, **98**, 187–193.
Zuo, L., Muller, J., Philippe, M.-J. & Esling, C. (1995). *Acta Cryst.* A**51**, 943–945.